

Extending matchgate simulation methods to universal quantum circuits

Avinash Mocherla¹, Lingling Lao^{1,2}, and Dan E. Browne¹

¹Department of Physics and Astronomy, University College London, United Kingdom

²School of Computer Science, Northwestern Polytechnical University, China

Matchgates are a family of parity-preserving two-qubit gates, nearest-neighbour circuits of which are known to be classically simulable in polynomial time. In this work, we present a simulation method to classically simulate an n -qubit circuit containing N gates, m of which are universality-enabling gates and $N-m$ of which are matchgates, in the setting of single-qubit Pauli measurements and product state inputs. The universality-enabling gates we consider include the SWAP, CZ, and CPhase gates. For fixed m as $n \rightarrow \infty$, the resource cost, T , scales as $O\left(\left(\frac{en}{m+1}\right)^{2m+2}\right)$. For m scaling as a linear function of n , however, T scale as $O\left(2^{2nH\left(\frac{m+1}{n}\right)}\right)$, where $H(\lambda)$ is the binary entropy function.

In quantum computing context, matchgates refer to a group of two-qubit parity-preserving gates of the form:

$$G(A, B) = \begin{pmatrix} a & 0 & 0 & b \\ 0 & e & f & 0 \\ 0 & g & h & 0 \\ c & 0 & 0 & d \end{pmatrix}$$

$$A = \begin{pmatrix} a & b \\ c & d \end{pmatrix}, B = \begin{pmatrix} e & f \\ g & h \end{pmatrix}$$

where $\det(A) = \det(B) = \pm 1$. Gates of this type commonly occur in domains such as quantum chemistry [1], fermionic linear optics [2], quantum machine learning [3], and comprise part of the native gate set of several quantum computing architectures. An important fact about matchgates is that when they are composed into nearest neighbour circuits, they are efficiently classically simulable. This was first discovered by Valiant [4] in the context of ‘perfect matchings’ of a graphical representation of matchgate unitaries. It was

then extended to a fermionic context by Terhal and DiVincenzo [5], and later Josza and Miyake [6], each of whom developed classical algorithms to efficiently simulate matchgate circuits in different input and output regimes. When confronted with the fact that matchgates are efficiently simulable, a natural question is whether such efficiency is maintained as small numbers of a universality-enabling primitive outside of the matchgate group are added. For example, such primitives could include CZ, SWAP and CPhase gates, which are all examples of ‘parity preserving non-matchgates’ [7], (for brevity we refer to these as ZZ gates). Is it possible to develop a method to simulate these universal matchgate circuits, dubbed ‘matchgate + ZZ’ circuits?

To answer this question we develop a Pauli-basis simulation method, which is able to simulate an n -qubit ‘matchgate + ZZ’ circuit containing m ZZ gates, in time which is polynomial in n when m is fixed, and scales as $\mathcal{O}(2^{2nH\left(\frac{m+1}{n}\right)})$ for $m \leq \frac{n}{2}$ in general, where $0 < H(\lambda) \leq 1$ is the binary entropy function. The use of a Pauli-basis method stems from the equivalence of fermionic and Pauli operator descriptions of matchgates via the Jordan Wigner representation. This allows us to succinctly represent the ‘matchgate + ZZ’ simulation problem in Liouville notation. In this notation, matchgate circuits manifest as block diagonal super-operators acting on closed (mostly poly-sized) linear spans of Pauli-operators. On the other hand, ZZ gates manifest as superoperators which act across several linear spans of Pauli operators. Given these two observations, classical simulation of matchgate + ZZ circuits is possible if, starting from a closed linear span, we adaptively keep track of the newly accessed Pauli basis elements as each ZZ gate is applied.

The paper is structured as follows. In section 1, we review the properties of matchgates rele-

vant to classical simulation. We introduce methods for simulating matchgate circuits from [6] and show how this formalism can be readily recast in Liouville notation. In Section 2, we extend these insights to non-matchgates and show how matchgates can in principle be simulated with any non-matchgate by considering the structure of the corresponding superoperators. In Section 3, we introduce the Pauli-basis simulation technique specifically for ‘matchgate + ZZ’ circuits, and in Section 4, determine its scaling in the regimes of fixed m and variable m . Finally, in Section 5, we verify the asymptotic scalings by performing numerical simulations of ‘matchgate + ZZ’ circuits arising in the Fermi-Hubbard model.

To begin, we introduce the salient properties of matchgates relevant to our discussion.

1 Review of Matchgate Simulation

Matchgates, which in quantum computing are gates of the form $G(A, B)$, where $\det(A) = \det(B) = \pm 1$, are closely associated with the dynamics of non-interacting fermions. This link stems from the fact that matchgates are the result of mapping a subset of so-called *fermionic Gaussian operations*, which arise in fermionic physics, to quantum computation. The fermionic setting allows us to understand why circuits of nearest-neighbour matchgates can be efficiently simulated and is the starting point of further analysis.

1.1 Gaussian operations

Consider a system of n fermionic modes with the k th mode associated with a creation and annihilation operator, a_k^\dagger and a_k respectively. It has been shown that there exists a mapping between these fermionic operators and spin- $\frac{1}{2}$ operators (Pauli matrices) via the Jordan Wigner representation. To demonstrate this map succinctly, it is useful to define a set of $2n$ hermitian operators $c_{2k-1} = a_k^\dagger + a_k$ and $c_{2k} = -i(a_k^\dagger - a_k)$, sometimes referred to as Majorana spinors, which pairwise satisfy the following anti-commutation relations for $\mu, \nu = 1, \dots, 2n$:

$$\{c_\mu, c_\nu\} \equiv c_\mu c_\nu + c_\nu c_\mu = 2\delta_{\mu\nu} I. \quad (1)$$

Using the Jordan-Wigner representation, each spinor can be written in terms of strings of Pauli

operators as follows:

$$\begin{aligned} c_{2k-1} &= \left(\prod_{i=1}^{k-1} Z_i \right) X_k \\ c_{2k} &= \left(\prod_{i=1}^{k-1} Z_i \right) Y_k. \end{aligned} \quad (2)$$

It is known that matchgates correspond to unitary operators generated from the set of nearest-neighbour operators $\mathcal{X} = \{X_k X_{k+1}, X_k Y_{k+1}, Y_k Y_{k+1}, Y_k X_{k+1}, Z_k, Z_{k+1}\}$. Using equation 2 we can see each of the elements of \mathcal{X} can be expressed as quadratic Majorana monomials:

$$Z_k = -i c_{2k-1} c_{2k},$$

for $k \in [1, \dots, n]$, and

$$X_k X_{k+1} = -i c_{2k} c_{2k+1}$$

$$Y_k Y_{k+1} = i c_{2k-1} c_{2k+2}$$

$$Y_k X_{k+1} = i c_{2k-1} c_{2k+1}$$

$$X_k Y_{k+1} = -i c_{2k} c_{2k+2}$$

This highlights that a matchgate is the *Gaussian operation*, $U_{MG} = e^{iH_{MG}}$ generated from a Hamiltonian H_{MG} which is a linear combination of quadratic monomials:

$$H_{MG} = -i \sum_{\mu \neq \nu = 2k-1}^{2k+2} \alpha_{\mu\nu} c_\mu c_\nu, \quad (3)$$

where $\alpha_{\mu\nu}$ is a real anti-symmetric matrix, and the spinors are drawn from the set $\{c_{2k-1}, c_{2k}, c_{2k+1}, c_{2k+2}\}$. The set consists of spinors that correspond to nearest-neighbour modes, specifically k and $k+1$. However, Gaussian operations can also be generated from quadratic monomials connecting non-nearest neighbour modes, such as $c_1 c_5$ or $c_2 c_6$, ie. from a more general Hamiltonian:

$$H = -i \sum_{\mu, \nu}^{2n} \alpha_{\mu\nu} c_\mu c_\nu. \quad (4)$$

Such monomials, expressed in terms of Pauli operators, act non-trivially across multiple qubits. It can be shown, however, that the Gaussian operation e^{iH} generated by H can be efficiently decomposed as a circuit of $\mathcal{O}(n^3)$ nearest-neighbour matchgates [6], when expressed in terms of qubits. Hence we can consider a general Gaussian operation to correspond to a nearest-neighbour matchgate *circuit*.

k	$L_2^{(k)}$	J-W-equivalent Paulis
0	I	II
1	c_1, c_2, c_3, c_4	XI, YI, ZX, ZY
2	$c_1c_2, c_1c_3, c_1c_4, c_2c_3, c_2c_4, c_3c_4$	$iZI, iYX, iYY, iXX, iXY, iIZ$
3	$c_1c_2c_3, c_1c_2c_4, c_1c_3c_4, c_2c_3c_4$	iIX, iIY, iXZ, iYZ
4	$c_1c_2c_3c_4$	$-ZZ$

Table 1: Spinor basis L_2 and Pauli basis P_2 for all values of $k \in [0, 4]$.

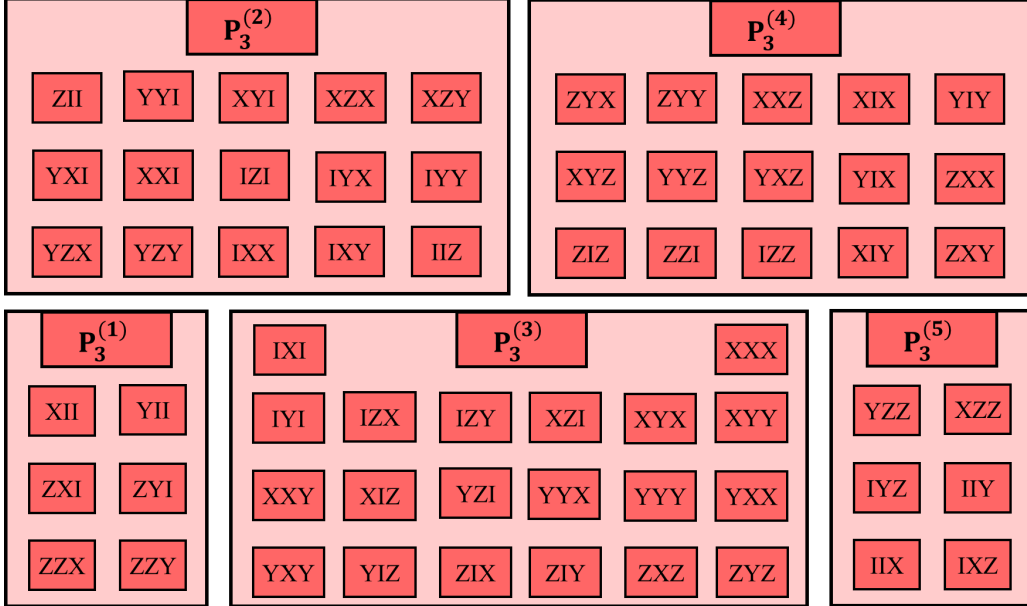


Figure 1: Subsets of P_3 . There are 5 subsets, denoted as $P_3^{(k)}$ each of size $\binom{6}{k}$. $P_3^{(0)} = III$ and $P_3^{(6)} = ZZZ$, as well as factors of i have been omitted for clarity.

1.2 PI-SO versus CI-MO simulation

Nearest-neighbour circuits of matchgates are well-known for their efficient classical simulability in specific input-output settings. The two primary settings are known as the PI-SO (product-input, single-output) and CI-MO (computational input, multi-qubit output) settings, as coined by Brod in [8]. In the PI-SO setting, computations involve nearest-neighbour matchgate circuits with product state inputs and measurements of single qubits. The simulation of such computations was established by Josza and Miyake [6], who exploited the Clifford algebraic properties of spinors (to be shown) to enclose the dynamics in a poly-sized vector space.

On the other hand, in the CI-MO setting, which focuses on computational basis states and measurements on subsets of output modes, it was demonstrated [5] that the marginal probability $p(y|x)$ for input and output bitstrings x and y can be efficiently evaluated. This was achieved

by reformulating the computation as the evaluation of the Pfaffian of an antisymmetric matrix, using Wick's theorem. Although both settings allow for efficient classical simulation, the underlying mechanisms behind their efficiency are not evidently related. Consequently, we direct our attention to the fundamental insights derived from the PI-SO setting and explore their applicability to universal circuits.

1.3 Clifford Algebra Formalism

While the spinors underlying the definition of matchgates have a natural fermionic interpretation, they can also be interpreted abstractly as the generators of a 2^{2n} dimensional Clifford algebra denoted \mathcal{C}_{2n} , as mentioned in [6]. The relevance of this observation to quantum computation is that the basis of \mathcal{C}_{2n} :

$$L_n = \{I, c_\mu, c_{\mu\nu} = c_\mu c_\nu, \dots, c_{12\dots 2n} = c_1 c_2 \dots c_{2n} \mid 1 \leq \mu < \nu < \dots \leq 2n\}, \quad (5)$$

reconstructed from unique ascending order products of spinors c_μ , forms a basis for $2^n \times 2^n$ hermitian matrices [9] [10]. Interestingly, such a property is also realised by the 2^{2n} dimensional n-qubit Pauli basis $\mathcal{P}_n = \{I, X, Y, Z\}^{\otimes n}$, and indeed, using the Jordan-Wigner representation, each element of L_n can be represented by an n-qubit tensor product of Pauli operators (up to a global phase). This is demonstrated in Table 1 for $n = 2$. An important consequence of this mapping is that the Pauli basis elements inherit the same graded structure as the underlying Clifford algebra. To make this clear, it is useful to label subsets of L_n by the degree of their constituent spinors, k , which we denote by $L_n^{(k)}$. The size of each of these sets is $\binom{2n}{k}$. There are $2n+1$ such sets (including $L_n^{(0)} = I$), and the linear span of the elements in $L_n^{(k)}$ is written as $\mathcal{L}_n^{(k)}$. We can see that as a vector space $\mathcal{C}_{2n} = \bigoplus_k \mathcal{L}_n^{(k)}$ and thus is graded. Each span $\mathcal{L}_n^{(k)}$ can be identified with a Pauli basis vector space $\mathcal{P}_n^{(k)}$ such that $\mathcal{P}_n = \bigoplus_k \mathcal{P}_n^{(k)}$. This structure is illustrated in Figure 1 for $n = 3$.

1.4 PI-SO Matchgate Simulation

We now show how this graded structure is exploited for classical simulation. Let us consider a typical computation in the PI-SO setting as the evaluation of the following expectation value:

$$\langle Z_j \rangle = \langle \psi | \mathcal{U}^\dagger(Z_j) \mathcal{U} | \psi \rangle, \quad (6)$$

where Z_j is the Z Pauli operator on the j th qubit, \mathcal{U} is the unitary denoting matchgate circuit with $N \sim \text{poly}(n)$ gates, and $|\psi\rangle$ is a product state. For a generic unitary, the classical resources required for this computation a priori scales exponentially. For a matchgate circuit, however, we can exploit the following key property of Gaussian operations, as shown by Jozsa and Miyake, to evaluate this expression in time $\text{poly}(n)$:

Theorem 1 [6] *Let H be a quadratic Hamiltonian as in 4 and $\mathcal{U} = e^{iH}$ the corresponding Gaussian operation. Then for all μ :*

$$\mathcal{U}^\dagger c_\mu \mathcal{U} = \sum_{\nu=1}^{2n} \mathcal{T}_{\mu\nu} c_\nu \quad (7)$$

where the matrix $\mathcal{T} \in SO(2n)$, and we obtain all of $SO(2n)$ in this way.

Proof 1 *Write c_μ as $c_\mu(0)$ and introduce $c_\mu(t) = V(t)c_\mu(0)V(t)^\dagger$ with $V(t) = e^{iHt}$. Then*

$$\frac{dc_\mu(t)}{dt} = i[H, c_\mu(t)]$$

(with square brackets $[a, b]$ denoting the commutator $ab - ba$). But $[c_{\nu_1}c_{\nu_2}, c_\mu] = 0$ if $\mu \neq \nu_1, \nu_2$ and $[c_\mu c_\nu, c_\mu] = -2c_\nu$ (from Equation 1) so

$$\frac{dc_\mu(t)}{dt} = \sum_{\nu} 4h_{\mu\nu}c_\nu(t)$$

$$c_\mu(t) = \sum_{\nu} \mathcal{T}_{\mu\nu}(t)c_\nu(0).$$

and the theorem follows by just setting $t = 1$.

Theorem 1 implies that conjugation by a Gaussian operation maps individual spinors to the closed real linear span of all spinors. Alternatively stated, conjugation by matchgate maps elements of $\mathcal{L}_n^{(1)}$ to $\mathcal{L}_n^{(1)}$. This applies to both matchgate circuits, \mathcal{U} , as well as individual matchgates U , as both are Gaussian operations. In each case, we will refer to the equivalent linear operator in $SO(2n)$ as \mathcal{T} and T respectively, and in general $\mathcal{T} = \prod_i^N T^{(i)}$ where $T^{(i)}$ is the linear operator for the i th gate in a circuit. As a corollary of Theorem 1, we can see that any degree monomial of spinors will be mapped to a linear span of the same degree, or equivalently the linear span $\mathcal{L}_n^{(k)}$ is preserved by conjugation of matchgates. Explicitly:

Corollary 1 *Let H be a quadratic Hamiltonian as in 4 and $\mathcal{U} = e^{iH}$ the corresponding Gaussian operation. Let S be any (ascending) order subset of $[0, 2n]$, and c_S be the monomial of spinors with indices in S . Then for all S with cardinality $|S|$:*

$$\mathcal{U}^\dagger c_S \mathcal{U} = \sum_{S' \in \binom{[2n]}{|S|}} \det(\mathcal{T}|_{S, S'}) c_{S'}, \quad (8)$$

where $\binom{[2n]}{k}$ denotes subsets of $[0, 2n]$ with cardinality k , and $\mathcal{T}|_{S, S'}$ indicates a minor of \mathcal{T} whose rows and columns are indexed by S and S' respectively.

The coefficients $\det(\mathcal{T}|_{S, S'})$ follow from applying the anti-commutation relations of the spinors, and are in fact the elements of a compound matrix $\mathcal{R}_n^{(|S|)} \in SO(\binom{[2n]}{|S|})$ for the given cardinality.

To understand how these results allow for efficient classical simulation in the PI-SO setting, let us rewrite Equation 6 using the fact that $Z_j = -ic_{2j-1}c_{2j}$:

$$\langle Z_j \rangle = -i \langle \psi | \mathcal{U}^\dagger c_{2j-1} c_{2j} \mathcal{U} | \psi \rangle.$$

Of immediate consequence is that the measurement operator $-ic_{2j-1}c_{2j} \in \mathcal{L}_n^{(2)}$. This suggests by conjugating the measurement operator, otherwise known as a ‘Heiseburg picture’ approach, we can write:

$$\langle Z_j \rangle = -i \sum_{S, S' \in \binom{[2n]}{2}} \det(\mathcal{T}|_{\{2j-1, 2j\}, S'}) \langle \psi | c_{S'} | \psi \rangle, \quad (9)$$

which is an expression which can be evaluated in polynomial time. This is due to the fact the sum consists of $\sim \mathcal{O}(n^2)$ terms, and for each term the determinant of constant-sized minors can be calculated efficiently from \mathcal{T} . Similarly, each expectation in the sum is the product of n single-qubit operator expectation values (as $|\psi\rangle$ is product state), which is also efficient. Hence by exploiting the fact that matchgates preserve the graded structure of the operator space, operators like $-ic_{2j-1}c_{2j}$ which start in a poly-sized vector space will remain in a poly-sized vector space.

1.5 Liouville notation

On the contrary, non-matchgates do not preserve the graded structure of the clifford algebra of spinors. In general, they act across several linear spans. To capture this behaviour, we recast the problem in the 4^n dimensional Pauli-basis via Liouville notation. Specifically, we can express a state ρ as a real column vector, which we refer to as an operator vector, $|\rho\rangle\rangle \in \mathbb{R}^{4^n}$,

$$|\rho\rangle\rangle = \left[\cdots \quad \rho_\sigma \quad \cdots \right]^T$$

where each vector element is the coefficient of the corresponding operator in its Pauli basis decomposition. That is,

$$\rho_\sigma = \text{Tr}(\sigma\rho)$$

Here, $\sigma \in P_n$ is an n -fold product of Pauli operators. We can also express an observable (i.e. Hermitian operator) M as a real row vector:

$$\langle\langle M | = \left[\cdots \quad M_\sigma \quad \cdots \right],$$

where each vector element is given by:

$$M_\sigma = \text{Tr}(\sigma M).$$

In this notation, the action of conjugation on the operator vector $|\rho\rangle\rangle$ is now given by a linear operator $R \in SO(4^n)$ acting on $|\rho\rangle\rangle$ denoted $|R|\rho\rangle\rangle$. Furthermore, the expectation value of an observable M can be written:

$$\langle M \rangle = \langle\langle M | R | \rho_0 \rangle\rangle, \quad (10)$$

which is equivalent to $\text{Tr}(MU^\dagger \rho_0 U)$ for a circuit U . Given that the objects in equation 10 are exponentially sized, a natural question is how such an expression can be evaluated efficiently. To do this, we introduce Algorithm A [see appendix A]. Algorithm A uses a sparse representation of each object to simulate the entire circuit in time which scales linearly in a quantity called χ_t . We define this below.

Definition 1 *The **Pauli rank** of $|\rho\rangle\rangle$, denoted $\chi(\rho)$, is the number of non-zero coefficients in its Pauli-basis decomposition.*

Definition 2 *The **Total Pauli rank** of a circuit-consisting of N gates, denoted χ_t , is the sum of the Pauli ranks obtained after applying each gate in the circuit. That is:*

$$\chi_t = \sum_i^N \chi(\rho_i). \quad (11)$$

Using Algorithm 1 on a matchgate circuit in the PI-SO setting, for example, we see that the maximum value of the Pauli rank (using a Heisenberg approach to matrix-vector multiplication) is $\chi = \binom{2n}{2}$. The total rank is, therefore, $\chi_t = N\chi$, which implies the scaling is the same as shown by Josza and Miyake in [6]. We will also make use of Algorithm 1 in evaluating the more general ‘matchgate + ZZ’ circuits introduced in the following sections.

2 Extension to non-matchgates

We now consider how non-matchgates manifest in the context of the graded structure of the Pauli-operator basis. To do this, we consider how non-Gaussian operations (ie. those generated by $H \in \mathcal{L}_n^{(d)}$ with $d \neq 2$) transform elements of a linear span $\mathcal{L}_n^{(k)}$ under conjugation. From this,

we can deduce the structure of the corresponding super-operator $R : \mathcal{C}_{2n} \rightarrow \mathcal{C}_{2n}$. What we find is that the application of such an operation induce transformations across *multiple* linear spans. This leads to a predictable increase in the Pauli rank of the measurement operator vector, allowing us to quantify the computational cost of simulating non-Gaussian operations. To relate non-Gaussian operations to unitary gates, we show that any single and two qubit gate: $U^{(1)} \in U(2)$ and $U^{(2)} \in U(4)$ respectively, can be reduced to two specific types of non-Gaussian operation. Namely, those operations generate odd-degree ad quartic elements of L_n respectively. We can hence characterise the classical cost of simulating any gate of practical relevance in terms of its effect on the Pauli rank of a simulation.

2.1 Transformations induced by non-Gaussian operations

To start, we note we can simplify our notion of non-Gaussian operations to those generated from $H \in L_n^{(k)}$, rather than $H' \in \mathcal{L}_n^{(k)}$, without loss of generality. This is from the observation that we can generate any element H' as $U^\dagger H U$, using Corollary 1 with a specially selected \mathcal{T} . The non-Gaussian operation generated from this new Hamiltonian, given by $e^{iU^\dagger H U}$ is equal to $U^\dagger e^{iH} U$, which implies that all non-Gaussian operations generated from $L_n^{(k)}$ are equivalent, up to conjugation by a matchgate, to the non-gaussian operation generated from the set $L_n^{(k)}$. We refer to this property as matchgate-equivalence.

Let us consider the transformation of a basis element $c_{\{k\}} \in L_n^{(k)}$, where through abuse of notation the subscript k refers to an (ascending order) subset of $[0, 2n]$ with cardinality k . We specifically consider the transformation $V^\dagger c_{\{k\}} V$, where V is a non-Gaussian unitary of the form $e^{i\frac{\theta}{2} c_{\{d\}}}$, and $c_{\{d\}} \in L_n^{(d)}$. Now, we have:

$$V^\dagger c_{\{k\}} V = \cos^2\left(\frac{\theta}{2}\right) c_{\{k\}} + \sin^2\left(\frac{\theta}{2}\right) c_{\{d\}} c_{\{k\}} c_{\{d\}} + i \sin\left(\frac{\theta}{2}\right) \cos\left(\frac{\theta}{2}\right) (c_{\{d\}} c_{\{k\}} - c_{\{k\}} c_{\{d\}}), \quad (12)$$

where it can be seen that the expression simplifies depending on whether the monomials $c_{\{d\}}$ and $c_{\{k\}}$ commute or anti-commute. Indeed, this depends on the number of sign flips induced by

rearranging $c_{\{d\}} c_{\{k\}} \rightarrow c_{\{k\}} c_{\{d\}}$, which is related to the values d, k and a quantity $l \in [0, \min(k, d)]$, which we define as $l = |\{k\} \cap \{d\}|$ (i.e. the number of spinors which occur in both $c_{\{d\}}$ and $c_{\{k\}}$):

Lemma 2 *Let k and d be the degrees of $c_{\{k\}}$ and $c_{\{d\}}$ respectively. Let $l = |\{k\} \cap \{d\}|$ be the number of spinor indices common to both. Then $c_{\{d\}} c_{\{k\}} = (-1)^{dk-l} c_{\{k\}} c_{\{d\}}$.*

Proof 2 *Majorana spinors anti-commute under permutation. This induces a sign depending on the number of permutations needed to transform $c_{\{k\}} c_{\{d\}} \rightarrow c_{\{d\}} c_{\{k\}}$. In the case $l = 0$ (no common spinors), the sign after this transform is $(-1)^{dk}$, as every spinor in $c_{\{k\}}$ is permuted past every spinor in $c_{\{d\}}$. When l is non-zero, l permutations will induce no sign (as these spinors will commute). Hence the overall sign induced after the full permutation is $(-1)^{dk-l}$.*

We can discern that in the commuting case ($dk - l$ is even), the transformation simplifies to the identity channel. However, in the anti-commuting case ($dk - l$ is odd), the following rotation occurs:

$$V^\dagger c_{\{k\}} V = \cos(\theta) c_{\{k\}} + i \sin(\theta) c_{\{d\}} c_{\{k\}}, \quad (13)$$

From equation 13, we see that non-matchgates transform $c_{\{k\}}$ to a space spanned by both $c_{\{k\}}$ and a monomial of the form $c_{\{d\}} c_{\{k\}}$. For a given value of l , $c_{\{d\}} c_{\{k\}}$ will simplify to $c_{\{d+k-2l\}}$, as two spinors with the same index will square to the identity. With these results, we can specify the linear span of the transformed monomial $V^\dagger c_{\{k\}} V$ as follows, depending on the values of d, k and l :

l parity	kd odd	kd even
l even	$\mathcal{L}_n^{(k)} \oplus \mathcal{L}_n^{(k+d-2l)}$	$\mathcal{L}_n^{(k)}$
l odd	$\mathcal{L}_n^{(k)}$	$\mathcal{L}_n^{(k)} \oplus \mathcal{L}_n^{(k+d-2l)}$

Table 2: Lookup table for the linear span to which $c_{\{k\}} \in L_n^{(k)}$ is transformed by a non-Gaussian operator of degree d , depending on the parity of l .

For a given d , $L_n^{(k)}$ will be split into l subsets, each of which will be transformed differently by a non-Gaussian operation V , according to Table 2. For an element of a *linear span* $\mathcal{L}_n^{(k)}$, which is a linear combination of basis elements $c_{\{k\}} \in L_n^{(k)}$,

we can say an element of $\mathcal{L}_n^{(k)}$ is transformed to the direct sum of the resultant linear spans of each transformed subset. To illustrate this, let us consider non-Gaussian operations corresponding to single- and two-qubit gates.

2.2 One-qubit non-Gaussian operations

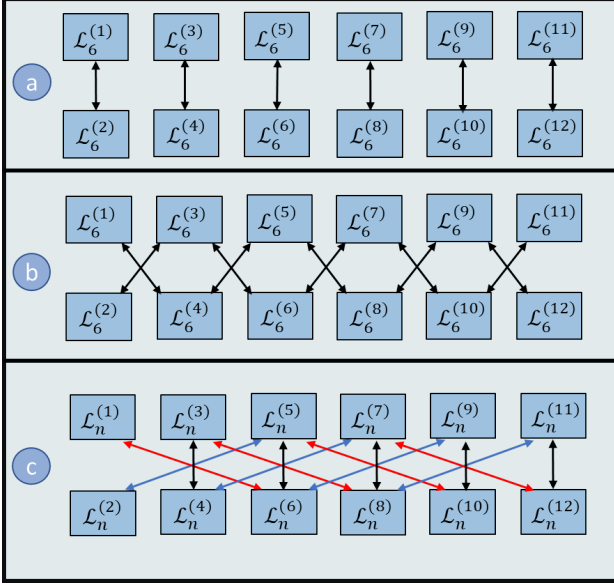


Figure 2: Transformation of an element of $\mathcal{L}_6^{(k)}$ under conjugation by an odd-degree non-Gaussian operation. Each arrow indicates the linear span to which a subset of $\mathcal{L}_n^{(k)}$ is transformed, corresponding to the possible values of l for that basis set. (a) $d = 1$, (b) $d = 3$, (c) $d = 5$ (Coloured arrows are for visualisation only).

Consider that any single-qubit gate can be decomposed, up to a global phase, as the product of three Euler rotations: $U^{(1)} = R_z(\theta_1)R_y(\theta_2)R_z(\theta_3)$, parameterised by angles $\theta_1, \theta_2, \theta_3$. The $R_z(\theta)$ rotations in this decomposition can be expressed as matchgates, because $G(R_z(\theta), R_z(\theta)) = R_z(\theta) \otimes \mathbb{1}$, which implies that the non-Gaussian component of a single-qubit rotation is contained in $R_y(\theta)$. We can say that single-qubit gates $U^{(1)}$ are *matchgate equivalent* to R_y gates.

An R_y rotation applied to qubit j can be expressed as $\cos(\frac{\theta}{2})I - i \sin(\frac{\theta}{2})Y_j$, where $Y_j = (-i)^{j-1} \prod_{i=1}^{j-1} (c_{2i-1}c_{2i})c_{2j}$. It can be seen that the R_y rotation is generated by *odd-degree fermionic operators*. Consider the simplest case where $j = 1$, which corresponds to a non-Gaussian operation of degree $d = 1$. The transformation induced on an element of $\mathcal{L}_n^{(k)}$ is given the following Theorem:

Theorem 3 Let $V = e^{i\theta c_{\{1\}}}$ be a degree 1 non-Gaussian operation. Then conjugation of an element of $\mathcal{L}_n^{(k)}$ by V is realized by a linear map $R_V^{(k)}$:

- For k odd:

$$R_V^{(k)} : \mathcal{L}_n^{(k)} \oplus \mathcal{L}_n^{(k+1)} \rightarrow \mathcal{L}_n^{(k)} \oplus \mathcal{L}_n^{(k+1)}$$
- For k even:

$$R_V^{(k)} : \mathcal{L}_n^{(k)} \oplus \mathcal{L}_n^{(k-1)} \rightarrow \mathcal{L}_n^{(k)} \oplus \mathcal{L}_n^{(k-1)}$$

Proof 3 For $d = 1$, the possible values of l are 0 and 1. This implies each set $L_n^{(k)}$ is composed of two subsets, each of which is transformed according to Table 2. Specifically, for $d = 1$,

$d = 1$	k odd	k even
$l = 0$	$\mathcal{L}_n^{(k)} \oplus \mathcal{L}_n^{(k+1)}$	$\mathcal{L}_n^{(k)}$
$l = 1$	$\mathcal{L}_n^{(k)}$	$\mathcal{L}_n^{(k)} \oplus \mathcal{L}_n^{(k-1)}$

When k is odd, it can be seen that for each value of l , an element of $\mathcal{L}_n^{(k)}$ is transformed to the linear span $\mathcal{L}_n^{(k)} \oplus \mathcal{L}_n^{(k+1)}$. Similarly, when k is even, an element of $\mathcal{L}_n^{(k)}$ is transformed to the linear span $\mathcal{L}_n^{(k)} \oplus \mathcal{L}_n^{(k-1)}$.

The structure of the linear operator $R_V : \mathcal{L}_n \rightarrow \mathcal{L}_n$, with the transformation due to each $R_V^{(k)}$ is shown graphically in figure 2a. Here each arrow represents the transformation of a subset of $L_n^{(k)}$ corresponding to a particular value of l (where a subset is transformed to its own linear span, no arrow is shown). It can be seen that under conjugation by a degree one non-Gaussian operator (which is matchgate-equivalent to a single-qubit gate on the first qubit), Theorem 3 corroborates a result in [11] which states that matchgates plus arbitrary single-qubit gates on the first qubit are efficiently classically simulable in the PI-SO setting. This can be seen by the fact that the measurement operator vector will contain terms in $\mathcal{L}_n^{(1)} \oplus \mathcal{L}_n^{(2)}$, as single-qubit gates will, under conjugation, induce transformations in the space $\mathcal{L}_n^{(1)} \oplus \mathcal{L}_n^{(2)}$. Separately, matchgates will induce transformations within the linear spans $\mathcal{L}_n^{(1)}$ and $\mathcal{L}_n^{(2)}$, which means that the overall Pauli rank will be bounded as $\binom{2n}{1} + \binom{2n}{2}$.

For odd-degree non-Gaussian operations corresponding to single qubit gates on higher indexed qubits, the transformations induced become more complicated, as shown in Figure 2b ($d = 3$) and

Figure 2c ($d = 5$). In these cases, efficient classical simulation is no longer possible as applying multiple single qubit gates interspersed with matchgates will in general induce transformation in the direct sum of linear spans which encompass an exponentially scaling portion of L_n .

2.3 Two-qubit non-Gaussian operations

To understand the transformations induced by two qubit gates, we make use of the fact that $U^{(2)} \in U(4)$ can be written (via a KAK decomposition [12][7]), in the following form:

$$U^{(2)} = (U_1 \otimes U_2) e^{i(aX \otimes X + bY \otimes Y + cZ \otimes Z)} (U_3 \otimes U_4).$$

Here the parameters a , b and c satisfy $a \geq b \geq c$ (to ensure the decomposition is unique.) Comparing this to the KAK decomposition for an arbitrary matchgate:

$$\left(e^{i\phi_1 Z} \otimes e^{i\phi_2 Z} \right) e^{i(aX \otimes X + bY \otimes Y)} \left(e^{i\phi_3 Z} \otimes e^{i\phi_4 Z} \right)$$

Comparing the two expressions, it can be seen that apart from the single qubit gates applied before and after the non-local core (which are matchgate-equivalent to R_y rotations), by elimination, the gate $U_{ZZ}(\theta) = e^{i\theta ZZ}$ must also induce non-Gaussian dynamics. Indeed, $U_{ZZ}(\theta)$ is a two-qubit parity-preserving gate which has been identified as enabling universal quantum computation when combined by Gaussian operations in [13], and corresponds to the unitary evolution of a degree four product of Majorana spinors. Specifically, when acting on qubits a and b (not necessarily nearest neighbour), one has $e^{i\theta Z_a Z_b} = e^{i\theta c_{2a-1, c_{2a}, c_{2b-1}, c_{2b}}$. It induces the following transformation on elements of $\mathcal{L}_n^{(k)}$:

Theorem 4 Let $U_{ZZ}(\theta) = e^{i\theta Z_a Z_b} = e^{i\theta c_{2a-1, c_{2a}, c_{2b-1}, c_{2b}}$ be a non-Gaussian gate acting on qubits a, b . Then for $n \geq 3$, conjugation of an element of $\mathcal{L}_n^{(k)}$ by U_{ZZ} is realized by a linear map $R_{ZZ}^{(k)}$:

- For $k \in [1, 2]$:

$$R_{ZZ}^{(k)} : \mathcal{L}_n^{(k)} \oplus \mathcal{L}_n^{(k+2)} \rightarrow \mathcal{L}_n^{(k)} \oplus \mathcal{L}_n^{(k+2)}$$
- For $k \in [3, 2n-2]$:

$$R_{ZZ}^{(k)} : \mathcal{L}_n^{(k-2)} \oplus \mathcal{L}_n^{(k)} \oplus \mathcal{L}_n^{(k+2)} \rightarrow \mathcal{L}_n^{(k-2)} \oplus \mathcal{L}_n^{(k)} \oplus \mathcal{L}_n^{(k+2)}$$

- for $k \in [2n-1, 2n]$:

$$R_{ZZ}^{(k)} : \mathcal{L}_n^{(k)} \oplus \mathcal{L}_n^{(k-2)} \rightarrow \mathcal{L}_n^{(k)} \oplus \mathcal{L}_n^{(k-2)}$$

Proof 4 For $d = 4$, the possible values of l are $0, 1, 2, 3, 4$. Hence the set $L_n^{(k)}$ consists of five subsets for each value of l . Given the product $4k$ is always even, we need only consider the even column of Table 2, for which we enumerate the following transformations:

$d = 4$	$4k$ even
$l = 0$	$\mathcal{L}_n^{(k)}$
$l = 1$	$\mathcal{L}_n^{(k)} \oplus \mathcal{L}_n^{(k+2)}$
$l = 2$	$\mathcal{L}_n^{(k)}$
$l = 3$	$\mathcal{L}_n^{(k)} \oplus \mathcal{L}_n^{(k-2)}$
$l = 4$	$\mathcal{L}_n^{(k)}$

For the first case where $k = 1$ or 2 , l is limited to be $0, 1$, or 2 . For any of these values, $\mathcal{L}_n^{(k)}$ is transformed to the linear span $\mathcal{L}_n^{(k)} \oplus \mathcal{L}_n^{(k+2)}$. For $k = 2n-1, 2n-2$: l can be either $l = 4, 3$ or 2 , which means $\mathcal{L}_n^{(k)}$ is transformed to $\mathcal{L}_n^{(k)} \oplus \mathcal{L}_n^{(k-2)}$. Finally, in the general case where l can be $0, 1, 2, 3$ or 4 , $L_n^{(k)}$ is transformed to $\mathcal{L}_n^{(k-2)} \oplus \mathcal{L}_n^{(k)} \oplus \mathcal{L}_n^{(k+2)}$.

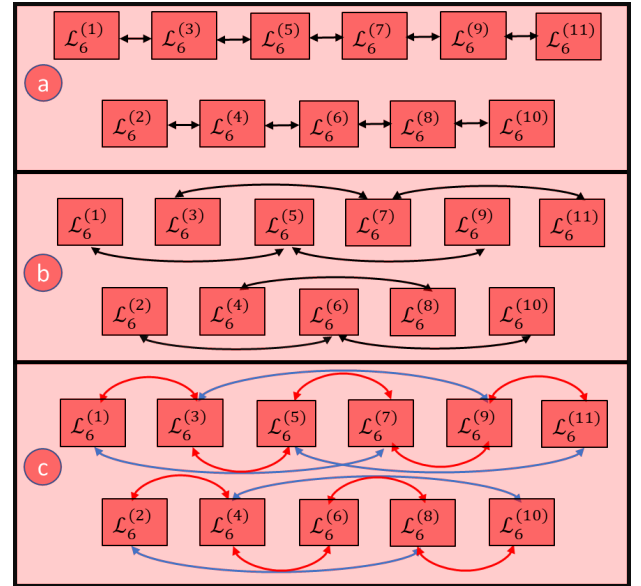


Figure 3: Transformation of an element of $\mathcal{L}_6^{(k)}$ under conjugation by an even-degree non-Gaussian operation. Each arrow indicates the linear span to which a subset of $\mathcal{L}_n^{(k)}$ is transformed, corresponding to the possible values of l for that basis set. (a) $d = 4$, (b) $d = 6$, (c) $d = 8$ (Coloured arrows are for visualisation only).

A schematic of the overall operation R_{ZZ} :

$\mathcal{L}_n \rightarrow \mathcal{L}_n$ is shown in Figure 3a. We can see that starting with a measurement operator vector in a given linear span, the action of conjugation, via the linear operator R_{ZZ} will in general access adjacent equal parity spans. This gives the scheme to simulate ZZ gates - keep track of the new basis elements which are accessed as each R_{ZZ} gate is applied, and update them as required. Such a method could be applied to any gate which is matchgate equivalent to U_{ZZ} including SWAP, CZ, and CPhase.

As well as these, the transformations induced by higher degree non-Gaussian operations, specifically $d = 6$ and $d = 8$ are shown in Figure 3 for completeness. In general, these would correspond to three and four-qubit gates in the Jordan-Wigner mapping and hence are not necessarily of practical relevance.

3 Classical Simulation of Matchgate + ZZ circuits

In the previous section, we showed how it is possible to simulate the action of a parity-preserving non-matchgate (a gate which is matchgate equivalent to U_{ZZ}) via the superoperator R_{ZZ} . Let us consider how adding such a gates affects the Pauli rank, and therefore the difficulty of simulation. We denote an n -qubit ‘matchgate + ZZ’ circuit containing N gates, of which m are parity-preserving non-matchgates and $N - m$ are matchgates, as U_{MG+ZZ} . This can be written in the following generic form:

$$U_{MG+ZZ} = U_{MG}^{(m)} U_{ZZ}^{(m)} \dots U_{MG}^{(1)} U_{ZZ}^{(1)} U_{MG}^{(0)}, \quad (14)$$

where there are $m + 1$ nearest-neighbour matchgate circuits U_{MG} interspersed with m U_{ZZ} gates.

A computation with this circuit in the PI-SO setting can then be written in Liouville notation as follows:

$$\langle Z_j \rangle = \langle \langle Z_j | R_{MG+ZZ} | \rho_0 \rangle \rangle. \quad (15)$$

where ρ_0 is a product state and $R_{MG+ZZ} = R_{MG}^{(m)} R_{ZZ}^{(m)} R_{MG}^{(m-1)} \dots R_{ZZ}^{(1)} R_{MG}^{(0)}$ are the corresponding superoperators. As has been mentioned, it is possible to evaluate an expression of the form of equation 15 using Algorithm 1. This will have a scaling of $\mathcal{O}(\chi_t)$. Hence, to determine the overall scaling of simulating a particular ‘matchgate + ZZ’ circuit, we must find suitable bounds on χ_t . This is the subject of the next section.

4 Bounds on simulation time costs

4.1 General bounds for $\chi_t(N, n, m)$

To begin bounding χ_t for a ‘matchgate + ZZ’ circuit, we assume that we apply the ‘Heisenberg picture’ approach to matrix multiplication and that our measurement vector contains terms solely in $\mathcal{P}_n^{(2)}$. With these assumptions, the application of m ZZ gates will at most access $m + 1$ linear spans of even parity, up to a maximum of $\lfloor \frac{n}{2} \rfloor - 1$. The simplest bound of χ_t is therefore $N \chi_{max}$, where χ_{max} is the sum of the sizes of each accessed linear span. Explicitly:

$$\chi_{max} = \sum_{i=1}^{m+1} |L_n^{(2i)}| = \sum_{i=1}^{m+1} \binom{2n}{2i}. \quad (16)$$

Such a partial sum has no closed form, and varies depending on whether m is fixed as a function of n or varies correspondingly. We consider both cases below.

4.1.1 Bounds for fixed m

If m is fixed in the above expression, we can show that the partial sum χ_{max} scales polynomially in n as $n \rightarrow \infty$:

Theorem 5 *The following relation holds:*

$$\chi_{max} = \sum_{i=1}^{m+1} \binom{2n}{2i} < \binom{2n}{2m+2} \frac{1}{1-r}, \quad (17)$$

where $r = (\frac{2m}{2n-2m-1})^2$.

Proof 5 *Consider that for $k < \lfloor \frac{p}{2} \rfloor$:*

$$\frac{\binom{p}{k} + \binom{p}{k-2} + \dots}{\binom{p}{k}} = 1 + \frac{k(k-1)}{(p-k+1)(p-k+2)} + \dots, \quad (18)$$

where the numerator of the left hand side is the partial sum we wish to bound. Notice that we can upper bound the right hand side above by:

$$1 + \left(\frac{k}{p-k+1}\right)^2 + \dots, \quad (19)$$

which is an infinite geometric series with ratio $r = (\frac{k}{p-k+1})^2$. This series converges to $\frac{1}{1-r}$, for $0 \leq r < 1$. Using the substitution that $p = 2n$ and $k = 2m + 2$, $r = (\frac{2m+2}{2n-2m-1})^2$ and the series converges as long as $0 \leq m \leq \lfloor \frac{n}{2} \rfloor - 1$. Rearranging equation 18 completes the proof.

Let us consider the asymptotic scaling as $n \rightarrow \infty$ with fixed m . We can see that in this limit, $r \rightarrow 0$, and the scaling is dominated by $\binom{2n}{2m+2}$. Hence we can conclude the following results, using the relation that $\binom{2n}{2m+2} < \frac{ne}{m+1} 2^{m+2}$, where e is Euler's constant:

Corollary 2 For fixed $m < m_c$, as $n \rightarrow \infty$, χ_{max} scales as $\mathcal{O}(\left(\frac{ne}{m+1}\right)^{2m+2})$.

This implies the total simulation cost of the algorithm, which is on the order of $\sim \mathcal{O}(\chi_t)$ will in the worst case scale polynomially in n , for fixed m .

4.2 Bounds for variable m

We have considered fixed m to this point. We now consider the scaling if m increases as a function of n in the limit where $n \rightarrow \infty$. We make use of the following bound, proved in [14], for this purpose:

Lemma 6 The following relation holds for $0 \leq k \leq n$:

$$S = \sum_{i=0}^k \binom{2n}{i} \leq 2^{2nH(\frac{k}{2n})},$$

where $H(x) = -x \log_2(x) - (1-x) \log_2(1-x)$ is the binary entropy function.

As we are only concerned with even terms of this sum we can make the following modification. Split S into even and odd terms $S = S_o + S_e$, where $S_o = \sum_{i=1}^{m+1} \binom{2n}{2i-1}$ and $S_e = \sum_{i=0}^{m+1} \binom{2n}{2i}$. Here, S_e is the quantity we wish to bound. The ratio $\frac{S_e}{S_o} = 1 + \frac{S_o}{S_e} = 1 + \mathcal{O}(n^{-1})$ to leading order, as the partial sum of . We can rearrange this expression to give a bound for S_e :

$$S_e \leq \frac{1}{1 + \mathcal{O}(n^{-1})} 2^{2nH(\frac{k}{2n})} \quad (20)$$

Finally, noting that $k = 2m+2$, We can bound χ_{max} in the asymptotic limit as follows:

Theorem 7 For $m \leq \lfloor \frac{n}{2} \rfloor - 1$:

$$\chi_{max} < 2^{2nH(\frac{m+1}{n})} \quad (21)$$

4.3 Tighter bounds for structured circuits

It is possible to give some tighter bounds on the simulation time complexity, if we assume some natural structure in the circuit. The motivation here is that the Pauli rank increases over

the course of the circuit instead of being fixed at χ_{max} . If the ZZ gates are equally spaced, we will have a staircase structure. Evaluating χ_t is then a question of splitting the staircase into horizontal steps and adding each section. In general the width of the k th step (starting from the bottom) each step will be $\frac{kN}{m+1}$, and the height will be $|L_{2k}|$. Hence we can approximate χ_t in the following way:

$$\begin{aligned} \chi_t(n, m) &\approx \\ &= \frac{N}{m+1} \sum_{i=1}^{m+1} (m+2-i) |L_n^{(2i)}| \\ &= \frac{N}{m+1} \sum_{s=1}^m (m+2-i) \binom{2n}{2i}, \end{aligned} \quad (22)$$

where $N = mT+m$, for some constant T which is the number of matchgates applied between each ZZ gate. This partial sum can be upper bounded by an arithmetico-geometric series as follows:

Lemma 8

$$\sum_{s=1}^{m+1} (m+2-i) \binom{2n}{2i} < \binom{2n}{2m+2} \left[1 + \frac{1}{(1-r)^2}\right], \quad (23)$$

where $r = \left(\frac{2m}{2n-2m+1}\right)^2$.

Proof 6 Consider that for $k < \frac{p}{2}$:

$$\begin{aligned} &\frac{\binom{p}{k} + 2\binom{p}{k-2} + 3\binom{p}{k-4} + \dots}{\binom{p}{k}} \\ &= 1 + 2 \frac{k(k-1)}{(p-k+1)(p-k+2)} + \dots \end{aligned} \quad (24)$$

We notice that we can bound this above by:

$$S_n = 1 + 2 \left(\frac{k}{p-k+1}\right)^2 + \dots, \quad (25)$$

which is an infinite arithmetico-geometric series with ratio $r = \left(\frac{k}{p-k+1}\right)^2$:

$$S_n = 1 + \sum_{i=1}^{\infty} (i+1)r^i \quad (26)$$

The sum converges to $\left[1 + \frac{1}{(1-r)^2}\right]$, for $0 \leq r < 1$. Using the substitution that $p = 2n$ and $k = 2m+2$, $r = \left(\frac{2m+2}{2n-2m-1}\right)^2$ and the series converges as long as $0 \leq m \leq \lfloor \frac{n}{2} \rfloor - 1$. The numerator of the fraction in equation 24 is equal to the partial sum we wish to bound. Hence rearranging this expression gives us the desired result.

We use this result in Theorem 9 to give a closed-form expression for a bound to χ_{max} .

Theorem 9 For $m \leq m_c = \lfloor \frac{n}{2} \rfloor - 1$:

$$\chi_{max}(n, m) < \frac{N}{m+1} \binom{2n}{2m+2} \left[1 + \frac{1}{(1-r)^2} \right], \quad (27)$$

which means for structured circuits there is an approximately $\frac{1}{m}$ improvement over the loose bound derived in the previous section.

5 Fermi-Hubbard Model Simulation using Pauli-basis Simulation

In this section, we demonstrate how a 'matchgate + ZZ' circuit arising in the context of the Fermi-Hubbard model can be simulated using Algorithm 1, and verify the above asymptotic scalings. The Fermi-Hubbard model is a widely used model in condensed matter physics to understand the properties of correlated fermionic systems. A 1D model consists of p sites, arranged in a line, with $q < 2p$ fermions distributed between these sites. Each site can contain a spin-up fermion, a spin-down fermion or both. Fermions can *hop* between adjacent sites, characterised by an energy J , and interact with a coulombic repulsion each other if a site is doubly occupied, characterised by an energy U . The Hamiltonian of the system is given below:

$$H_{FH} = -J \sum_{j=1}^{L-1} \sum_{\nu=\uparrow,\downarrow} a_{j,\nu}^\dagger a_{j+1,\nu} + \text{h.c.} + U \sum_{j=1}^L n_{j,\uparrow} n_{j,\downarrow}, \quad (28)$$

where the first term corresponds to hopping and the second term to the onsite interaction terms respectively.

Simulating this Hamiltonian can be achieved as follows. Firstly, the initial state is prepared using a Givens rotation circuit as shown in Figure 4c. This consists of a ladder of matchgates of the form G , for each electron being simulated. In this case, we consider two electrons. The parameters of each gate are chosen randomly for our purposes, though in practice they are carefully chosen to correspond to a Hartree-Fock state. Next,

the dynamics induced by H_{FH} are approximated using the Lie product formula:

$$e^{i(H_{hop}+H_{int})t} = \lim_{T \rightarrow \infty} \left\{ e^{iH_{hop} \frac{t}{N}} e^{iH_{int} \frac{t}{T}} \right\}^T,$$

which approximates the dynamics as the product of the individual hopping and interacting unitary operators, applied for a fractional amount of time. Each individual unitary can be decomposed as a circuit on $2n$ qubits, where the first and second register of n qubits correspond to spin up and spin down electrons respectively. The hopping terms are implemented as K rotations (also matchgate circuits) on each register, and the interaction terms is implemented as CPhase gates acting between registers. This is shown in Figure 4b. This process is repeated for a particular number of steps known as the trotter number T . This gives an overall circuit structure as shown in Figure 4a.

Writing the circuit explicitly, we can see that our circuit factorises into a form which is amenable to Algorithm 1: $U_{FH} = U_{MG}^{(T)} U_\phi^{(T)} \dots U_{MG}^{(1)} U_\phi^{(1)} U_{MG}^{(0)}$, where U_{MG} are matchgate circuits corresponding to the Givens and K rotations, and U_ϕ are CPhase gates. Indeed, CPhase gates are matchgate equivalent to $U_{ZZ} = e^{i\theta ZZ}$, specifically taking the form $\text{CPhase}(\theta) = e^{i\theta ZZ} G(R_z(2\theta), I)$. The fact that these gates act on distant qubits a and b poses no issue (in this case) as $R_z^a \otimes I$ and $I \otimes R_z^b$ be expressed as $G(R_z(\theta), R_z(\theta)) G(R_z(\theta), R_z(-\theta))$ respectively, and the transformations induced by $e^{i\theta Z_a Z_b}$ hold for any qubits a and b, according to Theorem 4.

To test Algorithm 1, we consider the simulation of Trotter circuits with limited interactions, where only a finite number of CPhase are present in each Trotter step. This corresponds to removing on-site interaction for particular sites in the Fermi-Hubbard model. This paradigm may be useful for error mitigation methods which use efficient simulation of 'training circuits' to understand and mitigate errors in a related universal circuit [15]. Typically, such training circuits would have to be from gate sets which are classically simulable but may not be functionally similar to the circuit being implemented. By extending the reach of classical simulation methods to universal circuits it is possible that such methods could perform better.

In Figure 5 we show the scaling of χ_{tot} (per

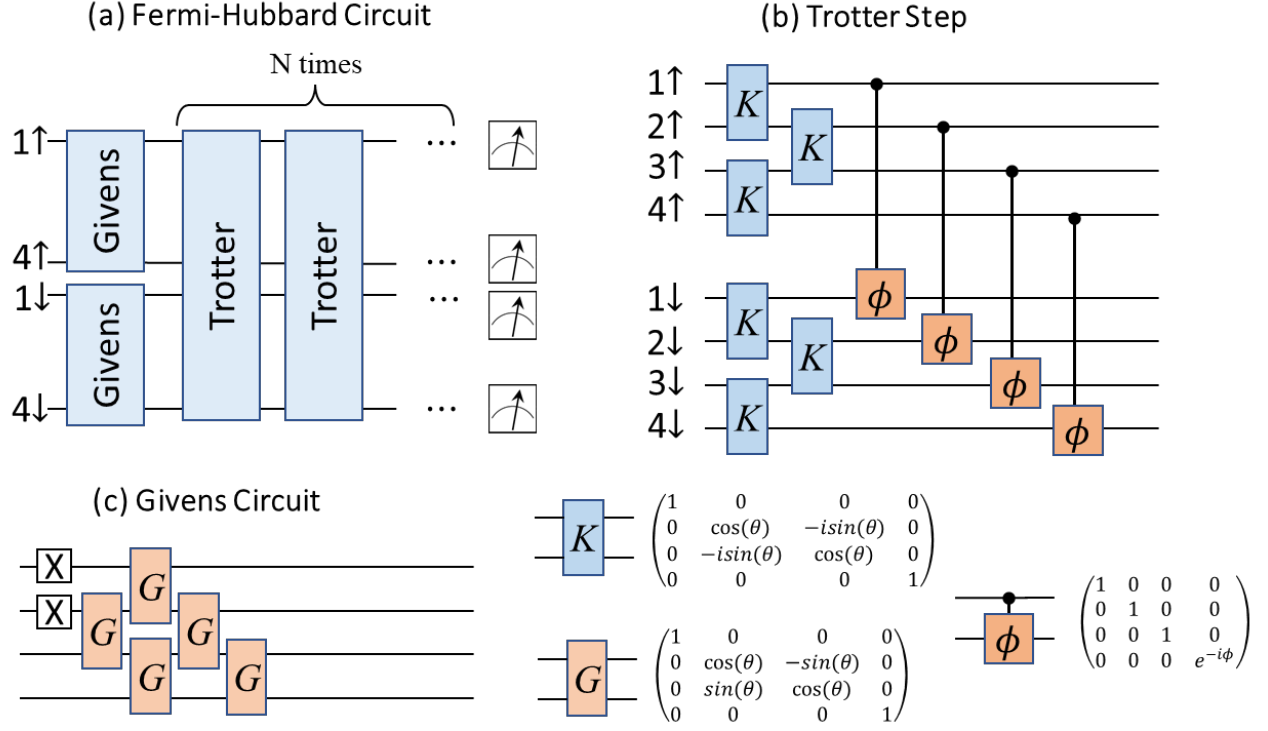


Figure 4: Circuit used to simulate time evolution of H_{FH} given in Equation 28, from [1]. (a) Overall circuit, consisting of initialisation of Hartree-Fock state using Given’s rotations as shown in (c). This is followed by m Trotter steps, and finally, measurement (b) Trotter step, consisting of odd-even hopping gates, even-odd hopping gates (blue) and onsite interactions (orange). In the interaction-limited case, only one cPhase gate connects the top and bottom registers.

gate) as a function of the number of Trotter steps (blue line), each step containing a single CPhase gate between the first qubit of the upper and lower register. In this case, the number of Trotter steps is equal to the number of parity-preserving non-matchgates. We simulate models consisting of $n_{sites} = 5, 10, 15$ sites (corresponding to $n = 10, 20, 30$ qubits respectively), for a number of Trotter steps T in the range $[0, 10]$. We further normalise the rank and time by the number of gates, the number of which is given by $N = 2n_{sites}(T + 1)$. From Figure 8, we verify our prediction that the simulator scales polynomially in the qubit number n , but exponentially in the number of parity-preserving non-matchgates. Furthermore, ignoring transient effects for small circuit depths, the time taken scales in proportion with the total Pauli rank.

5.1 Heuristic Improvements

We now mention two methods to improve the proposed simulation method. The first improvement is to use what is sometimes known as an *interac-*

tion picture approach, which describes applying R operators to both $|\rho_0\rangle\rangle$ and $\langle\langle Z_j|$. This reduces the number of iterations with a large number of multiplications which often occur in the final gates of a layered circuit. It also introduces parallelism as the two directions of multiplication can be computed independently. To initialise $|\rho_0\rangle\rangle$ using this method, one need only consider elements in the linear spans which will be accessed following the application of m parity-preserving non-matchgates gates. For computational zero states, this will be Pauli operators containing up to m Z operators.

The second method is to apply *pruning*, where coefficients from $\langle\langle M|$ which are below some threshold value ϵ are removed before the application of the next super-operator. At the cost of some error in the final expectation value, this heuristic has the potential to greatly reduce the time cost for certain circuits [see figure 5]. The relationship between the incurred error (δ) and the total pruning-free ($\epsilon = 0$) Pauli rank (per gate) is plotted in Figure 6. We consider the range of ranks accessed in our simulations, for different

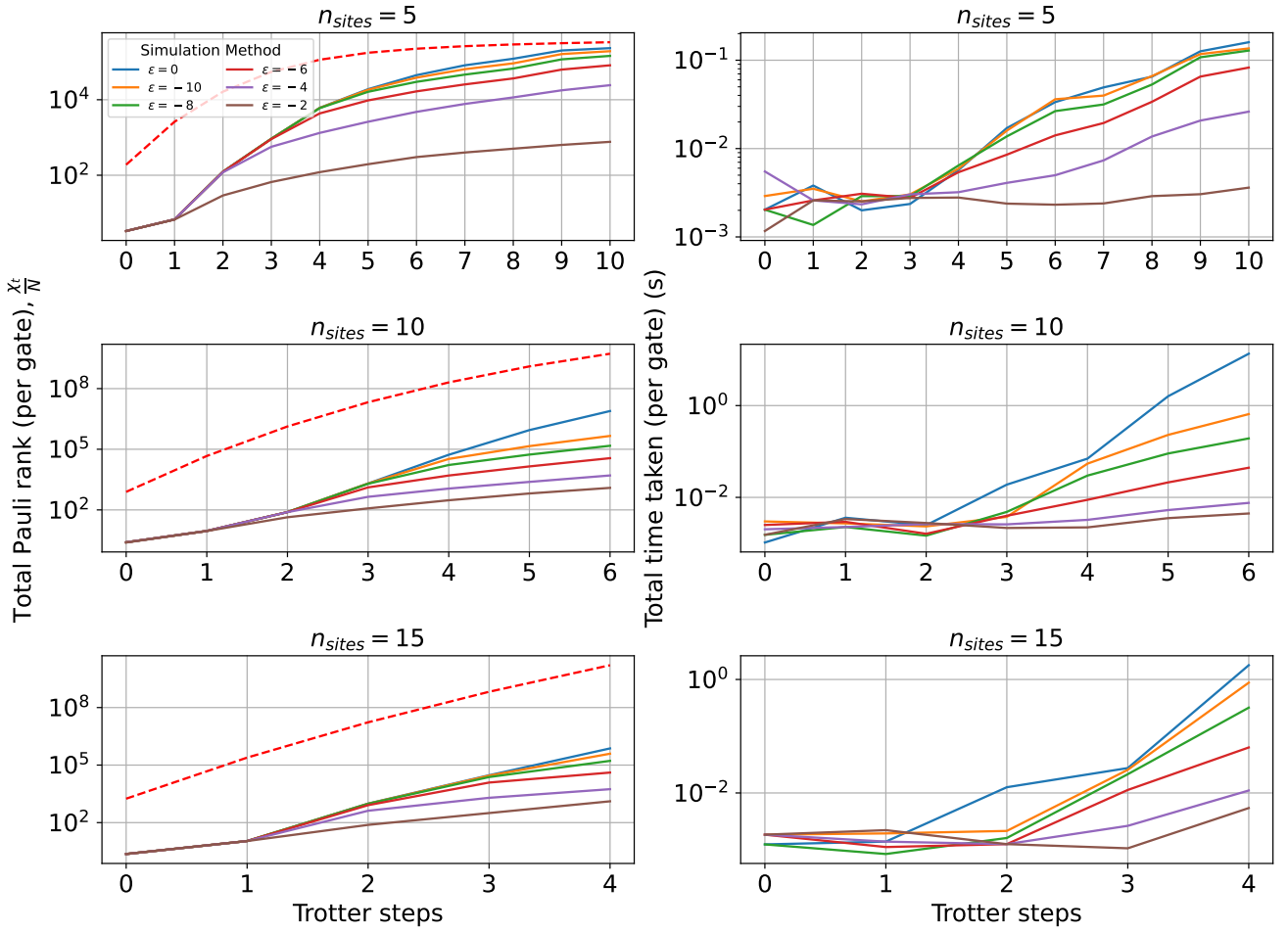


Figure 5: Total Pauli rank/Time (per gate) required to evaluate $\langle Z_j \rangle$ as a function of the number of Trotter Steps of an interaction limited version of the circuit shown in Figure 6. The red dashed line indicates the saturated upper bound for χ_t for the particular number of Trotter steps. For simulations with a pruning threshold, we can greatly reduce the simulation cost, however, we incur an error δ which varies as shown in Figure 6.

values of the pruning threshold (ϵ). Each point corresponds to a randomly initialised Trotter circuit with a particular value of n and T in the ranges $[4,7]$ and $[0,8]$ respectively. The same circuit is simulated for each value of the threshold ϵ .

6 Discussion

The motivating question for this research was whether the polynomial resource cost of nearest-neighbour matchgate circuit simulation techniques could be preserved for circuits supplemented with a few universality-enabling gates. Algorithm 1 shows that at the very least, poly-

nomial scaling is still possible for up to $\lfloor \frac{n}{2} \rfloor - 1$ such gates. As could be expected, the scaling quickly becomes exponential as more universality-enabling resources are added. It is however still possible that the exponent with respect to m could be suppressed with more sophisticated simulation techniques. For example, one line of research could be the use of tensor networks in simulating universal circuits [16]. In particular there are several schemes which efficiently encode fermionic gaussian states (ie states formed from matchgate circuits) as low-rank matrix-product states [17] [18]. We make note that there have recently been approaches which make analogies to the stabilizer decompo-

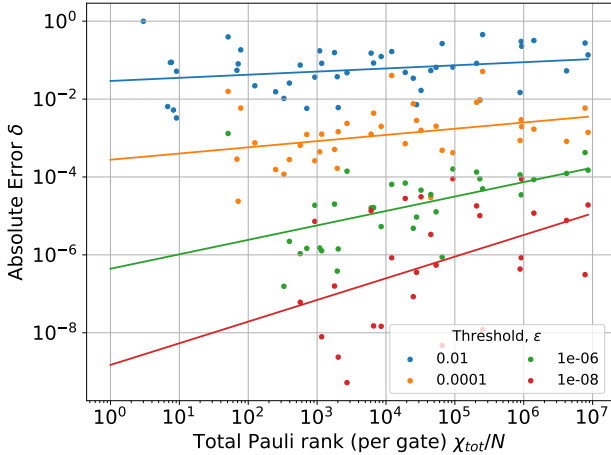


Figure 6: Absolute Error of expectation value for different values of pruning threshold, as a function of the total Pauli rank, χ_{tot} of a simulation. Each point corresponds to a Trotter circuit simulated with different values of n and T . The same set of circuits is used for each threshold value, and where the absolute error was zero, no point is shown.

sition approach. We direct the reader to these papers. [19]

We also mention here a few considerations for further investigation. Firstly, as the classical simulation results and scaling properties derived here stem from the fermionic description of operators, we can reason that using a different representation of these operators, such as the Bravyi-Kitaev, or a compact mapping for 2D fermionic grids [20], will lead to equivalent simulation methods for different sets of gates. Albeit such gates will no longer necessarily be nearest-neighbour matchgates or the identified parity-preserving non-matchgates. A detailed exposition of such gate sets is an interesting question.

7 Conclusion

In this paper, we have shown that it is possible to extend the PI-SO matchgate simulation method introduced by Jozsa and Miyake [6] to simulate a matchgate circuit containing a few parity-preserving non-matchgates (ZZ gates). At a high level, this is possible because of two observations. The first observation is that Gaussian operations induce linear transformation within a linear span $\mathcal{L}_n^{(k)}$, the vector space spanned by degree k majorana monomials. The second ob-

servation is that non-Gaussian operations induce transformations across *multiple* such linear spans. This gives a simple scheme to account for the addition of non-matchgates: adaptively increase the size of the vector space encompassing the dynamics over the course of a circuit. Using a sparse simulation method, we show that the time complexity of simulating a ‘matchgate + ZZ ’ depends on N , n , and m , the number of gates in total, the number of qubits and the number of ZZ gates. For $m \leq \lfloor \frac{n}{2} \rfloor - 1$, we show the time cost scales as $\sim \mathcal{O}(N(\frac{n}{m+1})^{2m+2})$ for fixed m as $n \rightarrow \infty$. For variable m , however, we find a scaling of the form $2^{2nH(\frac{m+1}{2n})}$. Finally, We showcase this method in a simulation of Trotter circuits arising from simulation of an interaction-limited Fermi-Hubbard model.

8 Acknowledgements

We would like to thank Daniel Brod for helpful discussions. We acknowledge funding from the EPSRC Prosperity Partnership in Quantum Software for Modelling and Simulation (Grant No. EP/S005021/1).

References

- [1] Frank Arute, Kunal Arya, Ryan Babush, Dave Bacon, Joseph C Bardin, Rami Barends, Andreas Bengtsson, Sergio Boixo, Michael Broughton, Bob B Buckley, et al. Observation of separated dynamics of charge and spin in the fermi-hubbard model. *arXiv preprint arXiv:2010.07965*, 2020.
- [2] Emanuel Knill. Fermionic linear optics and matchgates. *arXiv preprint quant-ph/0108033*, 2001.
- [3] Sonika Johri, Shantanu Debnath, Avinash Mocherla, Alexandros Singk, Anupam Prakash, Jungsang Kim, and Iordanis Kerenidis. Nearest centroid classification on a trapped ion quantum computer. *npj Quantum Information*, 7(1):1–11, 2021.
- [4] Leslie G Valiant. Quantum circuits that can be simulated classically in polynomial time. *SIAM Journal on Computing*, 31(4):1229–1254, 2002.
- [5] Barbara M Terhal and David P DiVincenzo. Classical simulation of noninteracting-

- fermion quantum circuits. *Physical Review A*, 65(3):032325, 2002.
- [6] Richard Jozsa and Akimasa Miyake. Matchgates and classical simulation of quantum circuits. *Proceedings of the Royal Society A: Mathematical, Physical and Engineering Sciences*, 464(2100):3089–3106, Jul 2008. ISSN 1471-2946. DOI: [10.1098/rspa.2008.0189](https://doi.org/10.1098/rspa.2008.0189). URL <http://dx.doi.org/10.1098/rspa.2008.0189>.
- [7] Daniel J. Brod and Ernesto F. Galvão. Extending matchgates into universal quantum computation. *Physical Review A*, 84(2), Aug 2011. ISSN 1094-1622. DOI: [10.1103/physreva.84.022310](https://doi.org/10.1103/physreva.84.022310). URL <http://dx.doi.org/10.1103/PhysRevA.84.022310>.
- [8] Daniel J. Brod. Efficient classical simulation of matchgate circuits with generalized inputs and measurements. *Physical Review A*, 93(6), Jun 2016. ISSN 2469-9934. DOI: [10.1103/physreva.93.062332](https://doi.org/10.1103/physreva.93.062332). URL <http://dx.doi.org/10.1103/PhysRevA.93.062332>.
- [9] David Hestenes and Garret Sobczyk. *Clifford algebra to geometric calculus: a unified language for mathematics and physics*, volume 5. Springer Science & Business Media, 2012.
- [10] Kianna Wan, William J Huggins, Joonho Lee, and Ryan Babbush. Matchgate shadows for fermionic quantum simulation. *arXiv preprint arXiv:2207.13723*, 2022.
- [11] Richard Jozsa, Barbara Kraus, Akimasa Miyake, and John Watrous. Matchgate and space-bounded quantum computations are equivalent. *Proceedings of the Royal Society A: Mathematical, Physical and Engineering Sciences*, 466(2115): 809–830, Nov 2009. ISSN 1471-2946. DOI: [10.1098/rspa.2009.0433](https://doi.org/10.1098/rspa.2009.0433). URL <http://dx.doi.org/10.1098/rspa.2009.0433>.
- [12] Barbara Kraus and Juan I Cirac. Optimal creation of entanglement using a two-qubit gate. *Physical Review A*, 63(6):062309, 2001.
- [13] Sergey B Bravyi and Alexei Yu Kitaev. Fermionic quantum computation. *Annals of Physics*, 298(1):210–226, 2002.
- [14] F. Jessie MacWilliams and N. J. A. Sloane. The theory of error-correcting codes. In *The Theory of Error-Correcting Codes*, 1977.
- [15] Ashley Montanaro and Stasja Stanisic. Error mitigation by training with fermionic linear optics. *arXiv preprint arXiv:2102.02120*, 2021.
- [16] Feng Pan and Pan Zhang. Simulating the sycamore quantum supremacy circuits. *arXiv preprint arXiv:2103.03074*, 2021.
- [17] Norbert Schuch and Bela Bauer. Matrix product state algorithms for gaussian fermionic states. *Physical Review B*, 100(24): 245121, 2019.
- [18] Matthew T Fishman and Steven R White. Compression of correlation matrices and an efficient method for forming matrix product states of fermionic gaussian states. *Physical Review B*, 92(7):075132, 2015.
- [19] Oliver Reardon-Smith, Michał Oszmaniec, and Kamil Korzekwa. Improved simulation of quantum circuits dominated by free fermionic operations. *arXiv preprint arXiv:2307.12702*, 2023.
- [20] Charles Derby, Joel Klassen, Johannes Bausch, and Toby Cubitt. Compact fermion to qubit mappings. *Physical Review B*, 104(3):035118, 2021.

A Algorithm 1

In this section, we introduce an algorithm to evaluate an expression of the following form:

$$\langle M \rangle = \langle \langle M | R | \rho_0 \rangle \rangle,$$

where $\langle \langle M |$ is a measurement operator vector, R is a superoperator corresponding to conjugation by a circuit, and $|\rho_0 \rangle \rangle$ is the initial density matrix vector. The algorithm can be shown to have a generic resource cost of $\mathcal{O}(\chi_t)$, where χ_t is the total Pauli rank of the circuit, as defined in equation 11. This algorithm could in theory be applied to a computation with any measurement operator, initial state or circuit, however we consider in what follows matchgate + ZZ circuits simulated in the PI-SO setting. Such circuits take the generic form:

$$U_{MG+ZZ} = U_{MG}^{(m)} U_{ZZ}^{(m)} \dots U_{MG}^{(1)} U_{ZZ}^{(1)} U_{MG}^{(0)}, \quad (29)$$

where there are $m + 1$ nearest-neighbour matchgate circuits U_{MG} interspersed with m U_{ZZ} gates. We remind the reader that many non-matchgates of practical relevance, such as SWAP, CZ and CPhase are matchgate equivalent to U_{ZZ} , and the matchgate components of these gates can be virtually absorbed into the neighbouring matchgate circuits, though in practice this isn't necessary. Recasting in Liouville notation, we can write the simulation problem explicitly as:

$$\langle Z_j \rangle = \langle \langle Z_j | R_{MG}^{(m)} R_{ZZ}^{(m)} \dots R_{MG}^{(1)} R_{ZZ}^{(1)} R_{MG}^{(0)} | \rho_0 \rangle \rangle, \quad (30)$$

where the superoperator corresponding to each matchgate circuit is written as R_{MG} . Furthermore, each $R_{ZZ}^{(m)}$ is the linear operator corresponding to a U_{ZZ} gate acting on arbitrary nearest neighbour qubits. To evaluate equation 30 efficiently, we use the 'Heisenberg picture' approach.. Furthermore, we use sparse data structures to ensure that no (initially) exponentially-sized object needs to be allocated to memory. Specifically, we can store $\langle \langle Z_j |$ during the computation as a dictionary of keys: $\langle \langle Z_j | = \{(P_1 : v_1), \dots, (P_\chi : v_\chi)\}$, where each key-value pair corresponds to a n -qubit Pauli operator and its coefficient in a Pauli-basis decomposition. Matrix-vector multiplication $\langle \langle Z_j' | R$ is then performed by (1), constructing the Pauli transfer matrix $O \in SO(16)$ for each gate, (2) cycling through each key in $\langle \langle Z_j' |$ and determining which basis elements are rotated by O , and (3) updating the corresponding values with matrix-vector multiplication.

To do step (1) efficiently, we use the observation that each R matrix is fully characterised by a rotation matrix $O \in SO(16)$ acting on a two-qubit subspace of Pauli operators, stemming from the fact that each gate is two-qubit. For each operator constituting an R_{MG} , the structure of O is a sparse block-diagonal with 1,4,6,4,1 dimensional submatrices corresponding to a rotation of the basis of $P_2^{(k)}$. The submatrices are calculated as shown in Subroutine 1. For R_{ZZ} , the corresponding O matrix can be calculated in constant time. For SWAP, for example, this will simply be a permutation matrix.

For step (2), we identify the elements of $\langle \langle Z_j' |$ which are rotated by each O matrix. To do this, we split every key into its *support* and a *stem* on qubits $j, j + 1$ denoted $P_{j,j+1}$ and $P_{n-j,j+1}$ respectively, describing the support of the key on the qubits j and $j + 1$, and its complement. The rotation will be the same for all keys with the same support. Hence, if $P_{j,j+1} \in P_2^{(d)}$, then the new basis elements following rotation are obtained by the tensor product of elements of $P_2^{(d)}$ with the stem (Subroutine 2).

As an example, consider a rotation supported on qubits 1 and 2. Then a key $ZIXY$ is split into ZI (support) and XY (stem). As the support is in $P_2^{(2)}$, the basis elements accessed in a rotation will be $ZIXY, IZXY, XXXY, YYXY, XYXY, YXXY$. We can store dictionary keys as integers by encoding n -qubit Pauli operator as a bitstring of size $2n$, where $I = 00, X = 01, Y = 10$, and $Z = 11$. Find(P) can then be efficiently implemented as integer addition and subtraction. Finally, we perform an update of the identified key-value pairs by performing a matrix-vector multiplication between the multiplication of the coefficients \vec{v} corresponding to \vec{P} (Subroutine 3).

The overall matrix-vector multiplication uses these three subroutines as shown in Algorithm 1. As the measurement vector is constantly being updated, it is important to keep track of which keys have already been rotated to avoid redundant multiplication. For this purpose, a separate data structure with $\mathcal{O}(1)$ write/read cost, labelled *temp* (such as a hash table) is used to store the keys already accessed using 'Find'.

The total simulation cost is proportional to a quantity denoted $\chi_t = \sum_i \chi_i$ which is the total sum of the Pauli ranks at each step of the circuit. The relevance of χ_t follows from the fact that the various contributions to the time cost are characterised by $\chi_i = \chi(Z_j')$ at each iteration. Specifically, the number of 'Find' and 'Update' calls for each gate can be approximated by $\frac{\chi_i}{s}$, where s is the maximum sparsity of each R matrix (which for R_{MG} is $s = 6$, and R_{ZZ} is $s=1$). Whereas 'Find' can be implemented as integer addition (which is efficient), matrix-vector multiplications during 'Update' calls will cost $\sim \mathcal{O}(s^2)$. Hence the dominant time cost for a single matrix-vector multiplication will be

$\mathcal{O}(\frac{\chi_i}{s} s^2) = \mathcal{O}(\chi_i s)$. Summing the costs across the entire circuit, the overall time cost will be $\mathcal{O}(\chi_t s)$. Hence, determining the overall time complexity of the algorithm reduces to finding suitable bounds for χ_t . Finally, we note that evaluating the final inner product scales as $\mathcal{O}(\chi_{max})$.

Subroutine 1: Rotations(U)

Input: U

Output: 1,4,6,4,1 dim matrices
 $R_{(0)}, R_{(1)}, R_{(2)}, R_{(3)}, R_{(4)}$

For $d \in [0, 4]$:

For $p_\alpha^{(d)}, p_\beta^{(d)}$ in $P_2^{(d)}$:

$$[R_{(d)}]_{\alpha\beta} = \text{Tr}(U^\dagger p_\alpha^{(d)} U p_\beta^{(d)})$$

Subroutine 2: Find(P)

Input: An n-qubit Pauli operator P , qubit indices $j, j+1$

Output: Subset of P_2, d

$$\vec{P} = \{P_1, \dots, P_m\} \text{ where } m = |P_2^{(d)}|,$$

support $\leftarrow P_{j,j+1} \in P_2^{(d)}$

stem $\leftarrow P_{n-(j,j+1)}$

For $p^{(d)} \in P_2^{(d)}$:

$$P_\alpha = P_{n-(j,j+1)} \otimes p^{(d)}$$

Subroutine 3: Update($\langle\langle M|, \vec{P}, R_{(d)}^i$)

Input: A set of keys \vec{P} , DofK $\langle\langle M|$

Output: Updated DofK $\langle\langle M|$

For $P_i \in \vec{P}$:

If $(P_i, v_i) \in \langle\langle M|$: $\vec{v} \leftarrow v_i$

Else: $\vec{v} \leftarrow 0$

$\vec{v} \leftarrow R_{(d)} \vec{v}$

$\langle\langle M| \leftarrow (\vec{P}, \vec{v})$

Algorithm 1: Sparse Pauli-basis simulation for 'Matchgate+ZZ' circuit

Inputs: Observable M , 'matchgate + ZZ' circuit: $U = U_{MG}^{(m)}U_{ZZ}^{(m)} \dots U_{MG}^{(1)}U_{ZZ}^{(1)}U_{MG}^{(0)}$ on n qubits, Initial product state ρ_0 .

Outputs: Expectation value $\langle M \rangle = \text{Tr}(U^\dagger M U \rho_0)$

Procedure:

Initialise measurement vector (e.g., $\langle\langle M | \leftarrow (Z_k : 1.0)$) as a dictionary of keys.

Matrix-vector Multiplication

For gates $U_{j,j+1}^{(i)} \in U_{MG}$ acting on qubits j and $j + 1$: $R_{(0)}^{(i)}, R_{(1)}^{(i)}, R_{(2)}^{(i)}, R_{(3)}^{(i)}, R_{(4)}^{(i)} \leftarrow$

Rotations $(U_{j,j+1}^{(i)})$

$temp \leftarrow \{\}$

For $(P^{(m)}, v^{(m)}) \in \langle\langle M |$:

If $P^{(m)} \notin temp$:

$\vec{P}, d \leftarrow \mathbf{Find}(P^{(m)})$

$\langle\langle M | \leftarrow \mathbf{Update}(\langle\langle M |, \vec{P}, R_{(d)}^{(i)})$

$temp \leftarrow \vec{P}$

Inner Product

For $(P_n^{(m)}, v_m) \in \langle\langle M |$: $\langle M \rangle += \text{Tr}(\rho_0 P_n^{(m)}) v_m$